

## An operational approach to real-time dynamic measurement of discharge

V. Alessandrini, G. Bernardi and E. Todini

### ABSTRACT

Based on the maximization of entropy, microwave sensors are becoming standard approaches for converting point surface velocity measurements into discharge. Unfortunately, this conversion is conditioned by cross-section regularity and by the need to take the surface measures above the vertical where the maximum velocity occurs. Cross-section irregularities and the presence of floodplains, vegetation and/or local bed depressions can change the theoretical applicability conditions of the proposed methods and, due to the wandering of the current, the microwave sensor must be continuously moved to track the maximum velocity. We describe the theoretical development and practical application of a new approach to operationally convert surface velocity and water level, measured using a fixed installation, into discharge. The resulting equation that links the surface point velocity measurement to the discharge is a function of two parameters describing the velocity distribution within the cross-section plus an additional correction factor which describes the non-homogeneity of the different vertical slices into which the cross-section is divided. Interesting results of the approach are shown for the gauging section of Tavagnasco on the Dora Baltea River in Italy with high performances both in terms of calibration and validation.

**Key words** | discharge measurements, entropy maximization, microwave surface velocity measurements, probabilistic approach

V. Alessandrini  
G. Bernardi  
Computer Application Engineering (CAE) SpA,  
Via Colunga 20,  
40068 San Lazzaro,  
Italy

E. Todini (corresponding author)  
Dipartimento di Scienze Biologiche,  
Geologiche e Ambientali (BiGeA),  
University of Bologna,  
Via Zamboni 67,  
40126 Bologna,  
Italy  
E-mail: ezio.todini@unibo.it

### INTRODUCTION

The instantaneous value of discharge in a canal or river cross-section of known geometrical characteristics can be represented as a function of the time-varying water depth  $y$  and average velocity  $v$ , namely  $Q = Q(y, v)$ . This implies both the water depth and the average cross-section velocity should be measured to correctly estimate the time-varying discharge. Today, apart from small rivers and canals where current meters are still used, flow measurements are generally made using Acoustic Doppler Velocity Profilers (ADCP), which allow the integration of the flow over the entire cross-section. Unfortunately, for safety reasons, ADCPs cannot be used during high flows and are mostly used to perform reference measurements. Discharge is still traditionally estimated as  $Q \cong Q(y)$  by means of a parametric function of the sole water depth which is known as the steady flow rating curve, or more simply the rating

curve. Rating curves are generally represented by monomial relationships such as  $Q = \alpha(y - \beta)^\gamma$  where  $\alpha$ ,  $\beta$  and  $\gamma$  are the parameters to be estimated on the basis of couples of  $y$  and  $Q$ , obtained via contemporaneous measurements of water depth and water velocity in the cross-section of interest.

These values are seldom measured during high flows, implying that the estimation of the parameters will only capture the low- and medium-flow values while the rating curve will be extended beyond the range of measurements. This 'extrapolation' beyond the range of measurements causes one of the major discharge estimation errors (Di Baldassarre & Montanari 2009), mainly dependent on parameter  $\gamma$  which controls the curvature of the rating curve. While smaller impacts on the flow estimation can be induced by other phenomena such as the seasonality in the vegetation,

another large cause of errors affecting discharge estimates using rating curves lies in the neglected unsteady flow effects. The combination of all these errors, particularly in large mild slope rivers, may easily reach 30% as shown by Di Baldassarre & Montanari (2009).

Driven by the emergence of new technologies and sensors, as well as by the interest of being able to describe unsteady flow discharges, in recent decades various methodological approaches have been proposed and tested to overcome the limitations induced by the use of steady-state rating curves. An example is the recent dynamic rating curve (DyRaC) (Dottori *et al.* 2009) approach, based on pairs of contemporaneous measures of water level in adjacent cross-sections of a river. DyRaC assumes a parabolic approximation of the Saint Venant equations and, by taking advantage of the link between the water surface slope and the average velocity, produces an estimate of discharge as a function of water depth and water surface slope, i.e.

$$Q \cong Q\left(y, \frac{\partial v}{\partial x}\right)$$

DyRaC requires two contemporary water depth measurements instead of the single measurement required by a traditional rating curve.

The advantage of DyRaC over the conventional monomial equations representing the steady-state rating curves is twofold. First of all, it directly allows estimation of the unsteady flow discharge, thus eliminating one of the major sources of errors. It offers another advantage in relation to the effect of extrapolation beyond the measurement range given that it exploits all the geometrical information of the two cross-sections where the water levels are measured and of an approximation of the energy losses in the reach in between.

The availability of new sensors based on microwaves has provided new opportunities of estimating the average cross-section velocity starting from the measurement of the surface velocity. The method was provided by the entropy theory such as that proposed by Chiu (1987, 1988) for open channels who established a bridge between the probability domain, where a probability distribution of the velocity is assumed, and the physical space, by deriving the cumulative

probability distribution function. The work of Chiu was followed by many authors (Yamaguchi & Niizato 1994; Moramarco & Singh 2001, 2008; Costa *et al.* 2006; Fulton & Ostrowski 2008; Moramarco *et al.* 2008, 2011; Ammari & Remini 2010; Brocca *et al.* 2010; Zasso 2010) who employed and tested the probabilistic approach under several conditions.

The advantage of the approach lies in the possibility of reliably converting a continuous time measure of surface velocity into an average cross-section velocity and into discharge, if associated with a simultaneous water level measurement. Unfortunately, the probabilistic approach was developed and tested on rather regular cross-sections and requires the surface velocity to be measured over the vertical where the maximum velocity in the cross-section occurs. This is certainly feasible using a movable microwave sensor when, for instance, performing reference measurements for calibrating a rating curve, but it is not possible in operational gauges. In the latter case, a fixed sensor is installed and cannot be moved to follow the continuous changes of the vertical where the maximum flow velocity occurs, which varies continuously due to the cross-section shape and the flow conditions.

This paper aims to tackle the above-mentioned problems and to demonstrate a potential use of the microwave sensors in combination with Chiu's probabilistic approach in operational practice.

## METHODOLOGY

### The probabilistic approach

The probabilistic approach stems from the principle of entropy maximization that has been used in several fields of research as a technique for deriving the probability density function of a random variable. The key concept is the principle that, in a physical system with certain assigned constraints, the entropy tends towards a maximum value as random events tend to occur in the greatest possible disorder.

Chiu (1987, 1988, 1989, 1991), Chiu & Murray (1992) and Chiu & Said (1995) formulated a probabilistic model based on the maximization of entropy in a cross-section of a

water course, deriving a two-dimensional velocity distribution of the form:

$$u = \frac{u_{\max}}{M} \ln \left[ 1 + (e^M - 1) \frac{\xi - \xi_0}{\xi_{\max} - \xi_0} \right] \tag{1}$$

where  $u$  is velocity in the longitudinal direction (orthogonal to the plane of the cross-section);  $M$  is a parameter measuring the entropy of the section;  $(\xi - \xi_0)/(\xi_{\max} - \xi_0)$  represents the spatial cumulative distribution of probability;  $\xi_{\max}$  is the value of  $\xi$  at the point of maximum velocity, i.e. where  $u = u_{\max}$ ; and  $\xi_0$  is the value of  $\xi$  at the point where  $u = 0$ .

The coordinate  $\xi$ , defined

$$\xi = Y(1 - Z)^{\beta_i} \exp(\beta_i Z - Y + 1), \tag{2}$$

is given as a function of two transformed coordinates  $Y$  and  $Z$ .  $Y$  and  $Z$  depend on the spatial coordinates  $y$  (vertical) and  $z$  (horizontal) by:

$$Y = \frac{y - \delta_y}{D - \delta_y - h}; Z = \frac{|z|}{B_i - \delta_i} \tag{3}$$

through appropriate parameters which take into account the water depth  $D$ ; the depth  $h$  at which the maximum speed occurs (positive if below the free surface or negative if above); the width of the section  $B$ ; and the eventual presence of elements that may modify the position of the zero reference plane (i.e. the point at which the velocity becomes zero). The parameters  $\beta_i$ ,  $B_i$  and  $\delta_i$  where  $i = 1, 2$  are respectively the exponent, the width at the surface and the displacement of the zero plane that apply to the left ( $i = 1$ ) and right ( $i = 2$ ) of the vertical at which the maximum velocity in the section is located.  $\delta_y$  is the displacement of the zero plane from the bottom. The need to introduce the displacement of the zero plane is strongly linked to the presence of local depressions, plants and vegetation or large rough elements in the river bed, which tend to significantly change the spatial distribution of the velocity field.

Note how the application of Equation (1) requires the calibration of up to 7 parameters:  $M$ ,  $h$ ,  $\delta_y$ ,  $\delta_1$ ,  $\delta_2$ ,  $\beta_1$ ,  $\beta_2$ . Such requirements are reduced to just two parameters. ( $M$ ,  $h$ ) if  $\delta_y$  can be assumed to be sufficiently small to be assumed null, i.e.  $\delta_y \cong 0$ , if  $\xi_0 = 0$  when velocity  $u = 0$ , if  $\xi_{\max} = 1$ ;

when velocity  $u = u_{\max}$  and if Equation (1) is specified in the vertical corresponding to the point where the maximum speed occurs in the section. This is identified by the vertical coordinate,  $z = 0$  from which Equation (2) becomes:

$$\frac{\xi - \xi_0}{\xi_{\max} - \xi_0} = \begin{cases} \frac{y/D}{1 - h/D} \exp\left(1 - \frac{y/D}{1 - h/D}\right) & \text{for } h \geq 0 \\ \frac{y}{D} \exp\left(\frac{1 - y/D}{1 - h/D}\right) & \text{for } h < 0 \end{cases} \tag{4}$$

where  $y$  is the vertical coordinate from the bottom of the section;  $D$  is water depth; and  $h$  is the depth of the point where the maximum speed is measured. The double expression for Equation (4) is because if  $h \geq 0$ , the maximum speed falls within the wet section and  $\xi_{\max} = 1$ ; when  $h < 0$  however the maximum speed falls above the wet section, and then

$$\begin{aligned} \xi_{\max} &= \frac{D/D}{1 - h/D} \exp\left(1 - \frac{D/D}{1 - h/D}\right) \\ &= \frac{1}{1 - h/D} \exp\left(-\frac{h/D}{1 - h/D}\right) \end{aligned} \tag{5}$$

Combining Equations (1) and (5), we obtain the result:

$$u = \begin{cases} \frac{u_{\max}}{M} \ln \left[ 1 + (e^M - 1) \frac{y/D}{1 - h/D} \exp\left(1 - \frac{y/D}{1 - h/D}\right) \right] & \text{for } h \geq 0 \\ \frac{u_{\max}}{M} \ln \left[ 1 + (e^M - 1) \frac{y}{D} \exp\left(\frac{1 - y/D}{1 - h/D}\right) \right] & \text{for } h < 0 \end{cases} \tag{6}$$

which describes the vertical profile of velocity and applies strictly only to the vertical in which the maximum in the section occurs.

Starting from the maximization of entropy Chiu (1988) and Chiu & Said (1995) show that, for the vertical in which the maximum velocity occurs, the following properties are true.

1. The average velocity ( $\bar{U}$ ) in the section is strictly proportional to the maximum speed recorded:

$$\bar{U} = u_{\max}^* \Phi(M) \tag{7}$$

in which  $u_{\max}^*$  is the maximum value of velocity over the vertical at which this maximum occurs (which therefore

corresponds to the maximum velocity in the entire cross-section). The value of the function  $\Phi(M)$ , defined:

$$\Phi(M) = \frac{e^M}{e^M - 1} - \frac{1}{M} \tag{8}$$

where the parameter  $M$  is a measure of the entropy of the section, and is constant for fixed  $M$ .

- The average velocity ( $\bar{U}$ ) in the section can also be expressed as a function of the average velocity ( $\bar{u}^*$ ) of the vertical in which the maximum velocity  $u_{\max}^*$  lies, defined:

$$\bar{u}^* = \frac{u_{\max}^*}{M} I(M, h/D) \tag{9}$$

which depends not only on the parameter  $M$  but also on the normalized distance  $h/D$  of the point where the speed is maximum from the free surface, which implies that the mean velocity along a vertical  $\bar{u}^*$  is not constant with respect to the water depth  $D$ . The function  $I(M, h/D)$  in Equation (9) is defined:

$$I(M, h/D) = \begin{cases} \int_0^1 \ln \left[ 1 + (e^M - 1) \frac{y/D}{1 - h/D} \exp \left( 1 - \frac{y/D}{1 - h/D} \right) \right] d(y/D) & \text{for } h \geq 0 \\ \int_0^1 \ln \left[ 1 + (e^M - 1) \frac{y}{D} \exp \left( \frac{1 - y/D}{1 - h/D} \right) \right] d(y/D) & \text{for } h < 0. \end{cases} \tag{10}$$

Substituting Equation (9) into Equation (7), we obtain:

$$\bar{U} = \bar{u}^* \frac{M\Phi(M)}{I(M, h/D)} \tag{11}$$

from which it can be noted that the ratio of the average speed of the overall section  $\bar{U}$  and that of the vertical where the maximum velocity occurs  $\bar{u}^*$  is not constant but varies as a function of the water depth  $D$ , unless  $h$  is proportional to  $D (h \propto D)$ , i.e. the ratio  $h/D = \text{constant}$ . In this case, for given values of  $M$  and  $h/D$ , the value of  $I(M, h/D)$  will be a constant independent of the value of  $D$ .

- Finally, the average velocity of the section  $\bar{U}$  can also be expressed as a function of the surface velocity  $u_D^*$

along the vertical where the maximum velocity occurs:

$$\bar{U} = \begin{cases} u_D^* \frac{M\Phi(M)}{\ln \left[ 1 + (e^M - 1) \frac{1}{1 - h/D} \exp \left( 1 - \frac{1}{1 - h/D} \right) \right]} & h \geq 0 \\ u_D^* \frac{M\Phi(M)}{\ln[1 + e^M - 1]} & h < 0 \end{cases} \tag{12}$$

since the relation between maximum speed  $u_{\max}^*$  along the vertical and the surface velocity  $u_D^*$  is given by:

$$u_{\max}^* = \begin{cases} u_D^* \frac{M}{\ln \left[ 1 + (e^M - 1) \frac{1}{1 - h/D} \exp \left( 1 - \frac{1}{1 - h/D} \right) \right]} & \text{for } h \geq 0 \\ u_D^* \frac{M}{\ln[1 + (e^M - 1)]} & \text{for } h < 0 \end{cases} \tag{13}$$

which, upon substitution into Equation (7), yields Equation (12).

Equation (12) allows the point velocity  $u_D^*$  recorded on the water surface over the vertical where the maximum velocity occurs, to be converted to the average flow velocity  $\bar{U}$  relevant to the entire cross-section. The average flow velocity can then be directly converted into the discharge  $Q = \bar{U}A(D)$ , knowing the wetted area  $A(D)[L^2]$  which is a function of the measured water depth  $D$ .

Many authors (Xia 1997; Moramarco & Singh 2001, 2008; Barbetta et al. 2002; Moramarco & Saltalippi 2002; Moramarco et al. 2004, 2008, 2011; Yamaguchi & Niizato 1994; Ammari & Remini 2010; Brocca et al. 2010; Zasso 2010) have shown that in a significant number of cases this characteristic is actually confirmed. However, the sections used by these authors tend to be quite regular and do not take into account abrupt variations in section, such as the berms, which tend to generate strong discontinuities in steady-state rating curve and require appropriate corrections (de Araujo Chaudhry 1998; Ardicioglu et al. 2005).

Moreover, although the estimated discharge can be effectively used for establishing and calibrating a rating curve in the cross-section, it is hardly usable for operational online measurements because of the need to continuously

adjust the surface flow sensor in order to follow the position of the vertical where the maximum flow velocity occurs (which varies continuously due to the cross-section shape and the flow conditions).

It is therefore necessary to find an alternative to Equation (12) to determine the average velocity (as well as the discharge) from the velocity now measured at a generic point over the water surface, possibly close to but not necessarily exactly, over the continuously wandering position of the vertical where the maximum velocity occurs.

First of all, it is interesting to note the relationship between the average velocity along the vertical where the maximum velocity  $\bar{u}^*$  occurs and the surface velocity  $u_D^*$  measured above the same vertical. This can be obtained by substituting Equation (13) into Equation (9):

$$\bar{u}^* = \begin{cases} u_D^* \frac{I(M, h/D)}{\ln \left[ 1 + (e^M - 1) \frac{1}{1 - h/D} \exp \left( 1 - \frac{1}{1 - h/D} \right) \right]} & \text{for } h \geq 0 \\ u_D^* \frac{I(M, h/D)}{\ln[1 + (e^M - 1)]} & \text{for } h < 0 \end{cases} \quad (14)$$

Many authors have suggested and verified the possibility of locally extending the validity of Equation (14) to other verticals characterized by a constant but not necessarily null Z coordinate (Greco 1999; Greco & Mirauda 1999; Moramarco et al. 2004; Burnelli et al. 2006; Zasso 2010). This implies that it is possible to write:

$$\bar{u}^i = \begin{cases} u_{D_i}^i \frac{I(M, h/D_i)}{\ln \left[ 1 + (e^M - 1) \frac{1}{1 - h/D_i} \exp \left( 1 - \frac{1}{1 - h/D_i} \right) \right]} & \text{for } h \geq 0 \\ u_{D_i}^i \frac{I(M, h/D_i)}{\ln[1 + (e^M - 1)]} & \text{for } h < 0 \end{cases} \quad (15)$$

Equation (15) shows how it is possible to convert the velocity  $u_{D_i}^i$  measured at the surface into the average speed along the corresponding  $i$ th vertical above which the measurement was taken. Note that in general the ratio of surface to average velocity will not be a constant but will vary as a function of the water depth  $D_i$ . However, under the reasonable assumption that the distance from

the free surface  $h$  at which the maximum velocity occurs is proportional to the water depth (namely  $h/D_i = \text{constant}$ ), it is easy to verify that the value of  $I(M, h/D_i)$  will also be a constant independent of  $D_i$ . Consequently, the ratio of average to surface velocities  $\bar{u}^i/u_{D_i}^i$  will also be constant, confirming the validity of one of the classic methods described by the US Geological Survey (Rantz et al. 1982).

### Extension of the equations to partialized cross-sections

Often it is necessary to take account of the presence of local depressions or vegetation at the bottom (Stephan & Gutknecht 2002) or, more generally, of the presence of rough elements of substantial size which effectively reduce the convective free area (Ferro & Baiamonte 1994; Ferro 2003). In these cases, the parameter  $\delta_y$  is no longer negligible and can no longer be regarded as null.

As shown in Figure 1, the velocity of flow in the lower part of the cross-section of depth  $\delta_y$  is almost zero, i.e.  $u^i \cong 0$  for  $0 \leq y \leq \delta_y$ , while for  $\delta_y \leq y \leq D_i$ ,  $u^i$  grows along the vertical with a law that follows Equation (6), rewritten

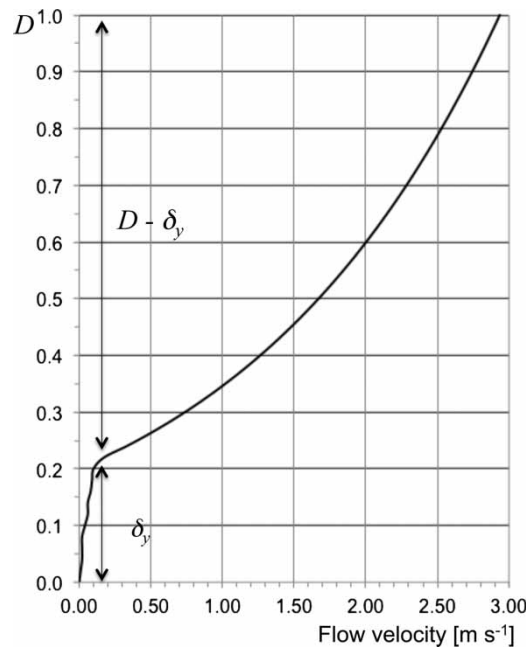


Figure 1 | The qualitative velocity profile due to bottom irregularities such as large rough elements, bottom depressions and underwater vegetation.  $\delta_y$  represents the 'displacement of the zero plane' and  $D$  the water depth.

to account for parameter  $\delta_y$ , usually referred to as the ‘displacement of the zero plane’:

$$u^i = \begin{cases} u_{D_i}^i \frac{\ln \left\{ 1 + (e^M - 1) \frac{(y - \delta_y)/(D - \delta_y)}{1 - h/(D - \delta_y)} \exp \left[ 1 - \frac{(y - \delta_y)/(D - \delta_y)}{1 - h/(D - \delta_y)} \right] \right\}}{\ln \left\{ 1 + (e^M - 1) \frac{1}{1 - h/(D - \delta_y)} \exp \left[ 1 - \frac{1}{1 - h/(D - \delta_y)} \right] \right\}} & \text{for } h \geq 0 \\ u_{D_i}^i \frac{\ln \left\{ 1 + (e^M - 1) \frac{(y - \delta_y)}{(D - \delta_y)} \exp \left[ \frac{1 - (y - \delta_y)/(D - \delta_y)}{1 - h/(D - \delta_y)} \right] \right\}}{\ln[1 + (e^M - 1)]} & \text{for } h < 0 \end{cases} \quad (16)$$

The average velocity along the vertical will therefore be the combination of the average velocity over the partition  $0 \leq y \leq \delta_y$ ,  $\bar{u}_{0-\delta_y}^i \cong 0$  which is practically null, and the average velocity over the partition  $\delta_y \leq y \leq D_i$  which is given by:

$$\bar{u}_{\delta_y-D_i}^i = \begin{cases} u_{D_i}^i \frac{I[M, h/(D_i - \delta_y)]}{\ln \left\{ 1 + (e^M - 1) \frac{1}{1 - h/D_i} \exp \left[ 1 - \frac{1}{1 - h/(D_i - \delta_y)} \right] \right\}} & \text{for } h \geq 0 \\ u_{D_i}^i \frac{I[M, h/(D_i - \delta_y)]}{\ln[1 + (e^M - 1)]} & \text{for } h < 0. \end{cases} \quad (17)$$

The average velocity is therefore:

$$\bar{u}^i = \bar{u}_{0-\delta_y}^i \frac{\delta y}{D_i} + \bar{u}_{\delta_y-D_i}^i \frac{D_i - \delta_y}{D_i} \cong \bar{u}_{\delta_y-D_i}^i \frac{D_i - \delta_y}{D_i}. \quad (18)$$

Consequently, the relationship between surface velocity and its average along the vertical is:

$$\bar{u}^i = \frac{D_i - \delta_y}{D_i} \begin{cases} u_{D_i}^i \frac{I[M, h/(D_i - \delta_y)]}{\ln \left\{ 1 + (e^M - 1) \frac{1}{1 - h/D_i} \exp \left[ 1 - \frac{1}{1 - h/(D_i - \delta_y)} \right] \right\}} & \text{for } h \geq 0 \\ u_{D_i}^i \frac{I[M, h/(D_i - \delta_y)]}{\ln[1 + (e^M - 1)]} & \text{for } h < 0. \end{cases} \quad (19)$$

Similarly to the case where  $\delta_y \cong 0$ , if  $h$  is assumed proportional to the height of the active section ( $D_i - \delta_y$ ) namely  $h \propto (D_i - \delta_y)$  the value of  $I[M, h/(D_i - \delta_y)]$  is independent of  $D_i$  for given values of  $M$  and  $h/(D_i - \delta_y)$ . We can therefore conclude that the average velocity along a vertical below the point of measurement is proportional to the surface velocity measurement according to:

$$\bar{u}^i = \frac{D_i - \delta_y}{D_i} \Psi u_{D_i}^i \quad (20)$$

where the value of the function  $\Psi = \Psi[M, h/(D_i - \delta_y)]$  does not depend on  $D_i$  once the values of parameter  $M$  and  $h/(D_i - \delta_y)$  are known.

### Extension of the equations to irregular cross-sections

Equation (20) allows the calculation of the average velocity  $\bar{u}^i$  on a strip around the  $i$ th generic vertical where the surface velocity is measured which, as previously stated, does not necessarily coincide with the vertical in which the maximum velocity occurs.

The problem now is to extend the local mean velocity along the  $i$ th vertical to the overall average velocity for the entire cross-section in order to calculate the discharge. This problem can be addressed using the same technique and assumptions generally used for the computation of the hydraulic conveyance in a cross-section.

To do so, the cross-section is divided into a number  $s$  of subsections (Figure 2) for which the head loss gradient  $J$  (also called friction slope) can be written:

$$J^{1/2} = \frac{n\bar{u}}{R^{2/3}(n)} \quad (21)$$

according to Manning’s equation. In Equation (21)  $R$  is the hydraulic radius of the cross-section and a function of the water depth  $D$ , and  $n$  ( $m^{-1/3} s$ ) is the Manning’s roughness coefficient.

Following Chow (1958), we can make the reasonable assumption that the friction slope is the same in all the vertical stripes, i.e.

$$J_j = J \forall j = 1, \dots, s \quad (22)$$



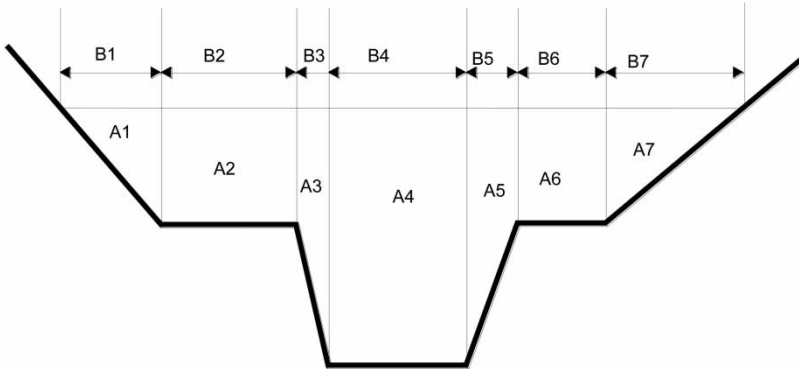


**Figure 2** | Example of subdivision of a cross-section into  $s$  subsections. In the figure,  $A_j$  indicate the wetted areas while  $B_j$  indicate the corresponding surface widths.

Subsequently, we can: (1) measure the surface velocity  $u_{D_i}^i$  over the  $i$ th subsection; (2) estimate the corresponding average velocity  $\bar{u}^i$  from Equation (20); and (3) compute the relevant friction slope  $J$ .

$$J^{1/2} = \frac{n_i \bar{u}^i}{R_i^{2/3}(D_i)} \tag{23}$$

At this point, we can deduce the average velocity in all the other subsections based on the Chow (1958) assumption that the friction slope remains constant over all other vertical subsections in which the overall section was divided, i.e.

$$\bar{u}^j = J^{1/2} \frac{R_j^{2/3}(D_j)}{n_j} \tag{24}$$

Computation of the overall discharge  $Q$  is then straightforward as the sum of all the subsection discharges:

$$Q = \sum_{j=1}^s A_j(D_j) \bar{u}^j \tag{25}$$

where  $A_j$  is the wetted area of the  $j$ th subsection, dependent upon the local water depth  $D_j$ . Substituting for  $\bar{u}^j$  from Equations (20) and (24) into Equation (25), we obtain:

$$Q = J^{1/2} \sum_{j=1}^s A_j(D_j) \frac{R_j^{2/3}(D_j)}{n_j} = \frac{n_i \frac{D_i - \delta_y}{D_i} \Psi u_{D_i}^i D_i}{R_i^{2/3}(D_i)} \sum_{j=1}^s \frac{A_j(D_j) R_j^{2/3}(D_j)}{n_j} \tag{26}$$

The dependence of overall discharge on the measured velocity  $u_{D_i}^i$  is evident from Equation (26). The ratio of the discharge  $Q$  to the velocity  $u_{D_i}^i$  measured at the surface of the  $i$ th subsection will not only vary linearly as a function of the water depth  $D_i$  of the measurement subsection, but also as a function of the hydromorphologic characteristics of all the other vertical subsections in which the original section has been divided.

From Equation (26) it is possible to analyse the effect of the non-homogeneity of the cross-section over the result of Equation (12) which, under the usual hypotheses, links the average velocity in the cross-section to the surface maximum velocity measurement through a constant. In the case of the new proposed approach, the average velocity can be written:

$$\bar{U} = Q/A(D) = \frac{D_i - \delta_y}{D_i} \Psi u_{D_i}^i \sum_{j=1}^s \frac{A_j(D_j) R_j^{2/3}(D_j)}{A(D) R_i^{2/3}(D_i)} \left(\frac{n_j}{n_i}\right)^{-1} \tag{27}$$

where  $\Psi$  is a constant as discussed above. The term  $[D_i - \delta_y/D_i]$  accounts for the eventual cross-section partialization, while the summation represents the additional correction factor which accounts for the non-homogeneity of the cross-section. This correction factor is a weighted sum, with weights  $[A_j(D_j)/A(D)]$  of the ratio raised to 2/3 of the individual subsection hydraulic radius to that of the subsection where the measurement is taken, i.e.  $[R_j^{2/3}(D_j)/R_i^{2/3}(D_i)]$  times the inverse of the analogous ratio of roughness coefficients  $[(n_j/n_i)^{-1}]$ . While the

weights and the hydraulic radius ratios can be determined from the geometrical description of the cross-section, the roughness coefficients have to be determined from the analysis of the rough elements characterizing the cross-section: silt, gravels, rocks, concrete, vegetation, etc. In principle the number of these parameters, the Manning's  $n$  coefficients, could be large as  $s$ , the number of subsections. In reality, the number can be very small: for instance one value describing the river bed and one describing the berms. Following a common practice in hydraulic 1D/2D modelling, the roughness coefficients can be attributed according to tables (Chow 1958) following a physical interpretation of rough elements instead of being estimated as parameters, which would increase the degrees of freedom and the indetermination of the final results. Note that it is not the actual friction value that matters but a relative value expressing how rough the subsection is with respect to the one where the measurement is taken. This clearly reduces the relevance of the roughness coefficient values to the overall correction factor, as experienced by the authors.

The two correcting effects are clearly fundamental in order to reproduce the low flows, while their effect will tend to vanish as soon as the water levels will be sufficiently high that the overall cross-section will contribute to the flow.

## TEST SITE AND DATA

The validity of the proposed methodology was tested at the gauging section of Tavagnasco (Figure 3) of the Dora Baltea, a river in north Italy. The gauging station traditionally includes a water level gauge and a steady-flow rating curve. Figure 4 shows the measurement cross-section and the location of the surface velocity sensor over the second arch of the bridge.

The calibration of equations was performed using couples of values of level and surface discharge recorded every half hour during the period 20 June–19 October 2010 when the discharge never exceeded  $320 \text{ m}^3 \text{ s}^{-1}$ . Verification of results was performed on data from the period 22 October–21 November 2011, in which the maximum discharge exceeded  $600 \text{ m}^3 \text{ s}^{-1}$ .



**Figure 3** | The cross-section of Tavagnasco on the Dora Baltea in Italy where the sensor was installed (top) and a detail of water level and surface velocity sensors (bottom) used for flow measurements.

## RESULTS AND DISCUSSION

Calibration was performed as follows. Values of the Manning's roughness coefficients for the different subsections were initially established on the basis of values suggested in the literature (Chow 1958; Barnes 1967). Two basic values of Manning's roughness coefficient were used: the value of  $n = 0.045$  was used to represent the presence of rough material in the lower part of the cross-section and the vegetation on the lateral sides, while the value of  $n = 0.035$  was used elsewhere.

Calibration was performed by setting  $\delta_y = 0$  and by adjusting the proportionality coefficient  $\Psi$  (Equation (21)) in order to match the computed discharge values to the steady-flow rating curve values. The resulting parameter values of  $M = 8$  and  $h = 0$  led to the value of  $\Psi = 0.82$  as



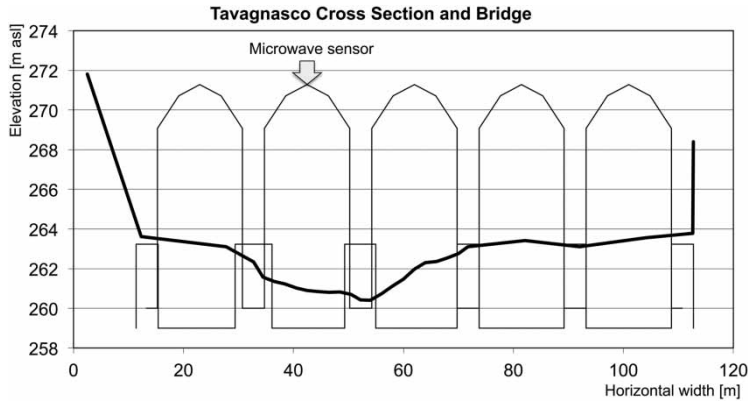


Figure 4 | The Tavagnasco measurement cross-section in the Dora Baltea also showing the bridge. The arrow indicates the position of the microwave sensor.

well as to a good agreement for higher values, but all the lower discharge values were increasingly overestimated. This was found to be caused by the presence of a local river bed depression as typically occurs in the proximity of bridge piers. The lowest point at 260.40 metres above sea

level (m.a.s.l.) was far below 262.90 m.a.s.l., the bed elevation at a nearby downstream cross-section. This distorts the relationship between surface velocity measure and average cross-section velocity, thus requiring the introduction and the estimation of a variable displacement of the zero plane  $\delta_y$ . When the water level falls below the downstream higher bed elevation the flow vanishes because, regardless of the surface velocity measurement, the active cross-section is zero ( $\delta_y = D$ ). When water level and flow increase,  $\delta_y$  rapidly tends to zero following the increase in active cross-section. Consequently, the displacement of the zero plane  $\delta_y$  was assumed to be represented by  $\delta_y = D \exp(-\alpha D)$ ; the results shown in Figure 5 were obtained from the estimated value for  $\alpha = 3$ .

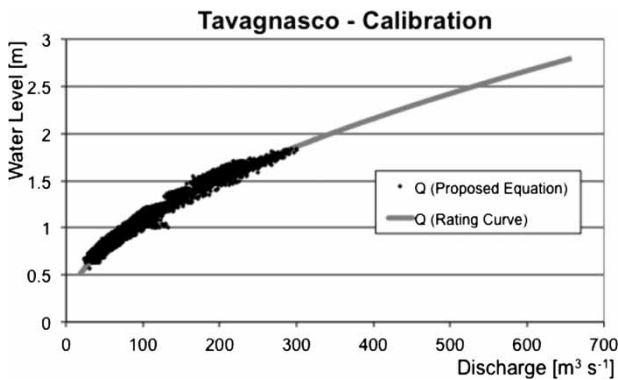


Figure 5 | The measured water level and discharge couples, estimated after calibrating the proposed approach in the period 20 June–19 October 2010, are plotted against the available steady-flow rating curve.

Apart from modest differences due to the unsteady flow induced by the daily releases of an upstream reservoir as opposed to the steady-flow nature of the discharge obtained using the rating curve, the match can be considered satisfactory. Figure 6, which provides a comparison of discharge

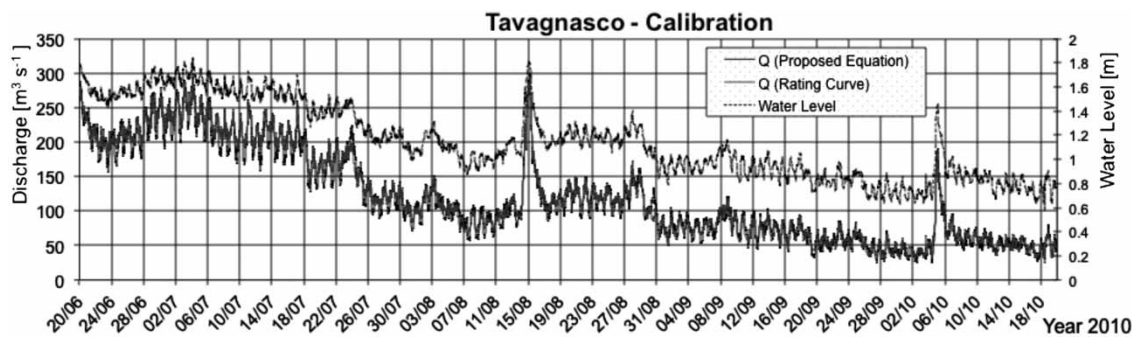
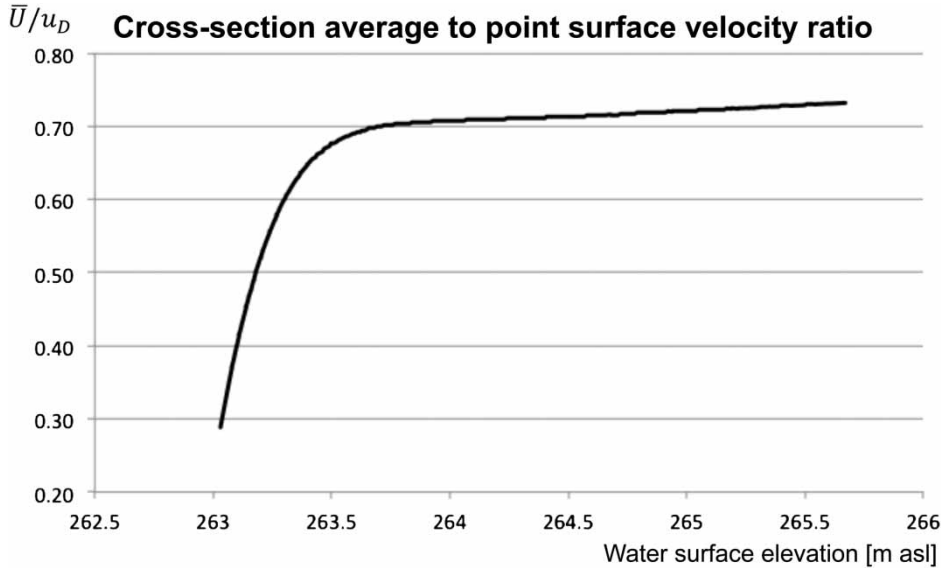


Figure 6 | Comparison of the discharge estimates based on the steady-flow rating curve available at Tavagnasco gauging station on the Dora Baltea in Italy and the corresponding values estimated on the basis of the proposed approach in the calibration period of 20 June–19 October 2010.



**Figure 7** | Ratio of the surface point velocity measurements to the overall average cross-section velocity. It can be seen that the value lies at c. 0.72–0.73 for the higher water levels values, while drops rapidly when the water level is below 263.7 m.a.s.l. which corresponds to the lower part of the cross-section (Figure 4).

estimated using the proposed approach and the discharge obtained using the steady-state rating curve, confirms the quality of the discharge estimates.

The resulting ratio of the observed surface velocity to the average cross-section velocity is depicted in Figure 7 which demonstrates that it is more or less constant at around 0.73 at higher water level values, while rapidly dropping when the water level approaches 262.90 m.a.s.l.

As can also be seen in Figures 8–10, the validation results are more than satisfactory. Figure 8 shows that there is noticeable agreement between the steady-flow rating curve values and the values obtained using the calibrated Equation (26). Note that the minor differences mostly arise from the fact that the proposed approach, as opposed to the steady-flow rating curve, produces a mild loop rating curve. The same quality of results in terms of discharge matching can be observed in Figures 9 and 10, the latter providing a more detailed view of the behaviour during high flows.

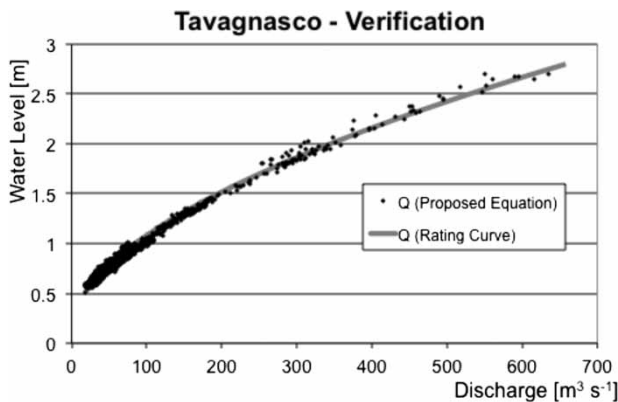


**Figure 8** | The measured water level and discharge couples obtained with the proposed approach are plotted for the verification period 22 October–21 November 2011 against those obtained using the available steady-flow rating curve. There is a noticeable agreement between the two. Note that the minor differences arise from the fact that the proposed approach, as opposed to the steady-flow rating curve, produces a mild loop rating curve.

## CONCLUSIONS

Additional extensive testing of the approach to determine any potential problems and pitfalls is needed. It can however be concluded from the application example that the original algorithm, which assumed a constant ratio of maximum velocity in one river cross-section to average velocity, can be extended with simple changes to complex river sections including floodplains (where irregularities of the riverbed exist in the form of large rough elements, submerged vegetation and local depressions). This work also demonstrates the possibility of installing operational

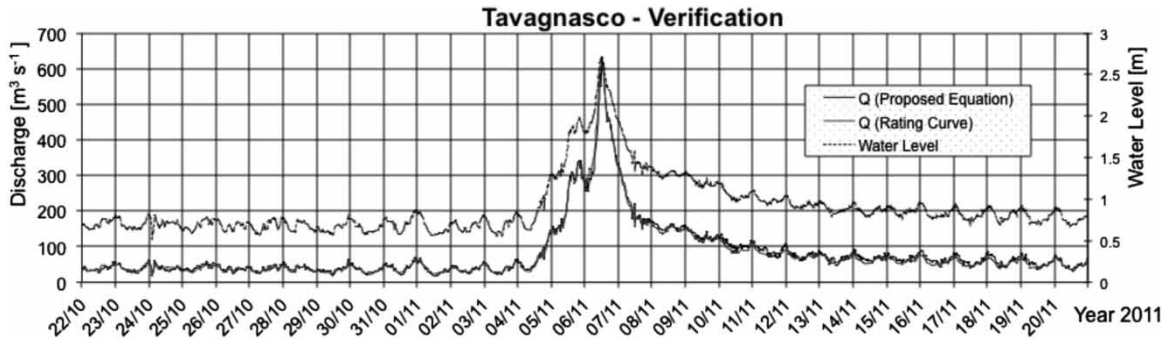


**Figure 9** | Verification period 22 October–21 November 2011. Comparison of the discharge estimates based on the steady-flow rating curve available at Tavagnasco gauging station on the Dora Baltea in Italy and the corresponding values estimated on the basis of the proposed approach. The results demonstrate a noticeable agreement not only during the flood event but all along the flow record.

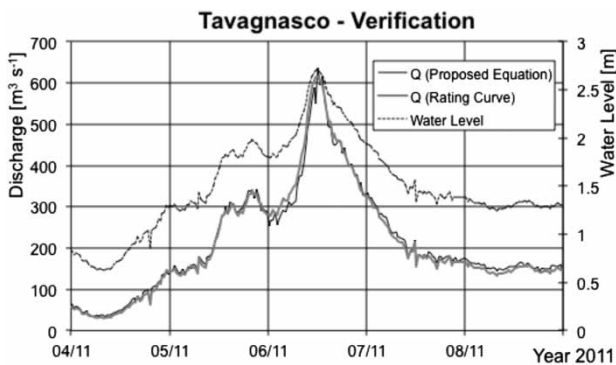


**Figure 10** | A detail of the verification for the high flows observed in the period 4–9 November 2011. Comparison of the discharge estimates based on the steady-flow rating curve available at Tavagnasco gauging station on the Dora Baltea in Italy and the corresponding values estimated on the basis of the proposed approach, demonstrating a noticeable agreement.

systems for continuous-time unsteady-flow discharge measurements based on fixed instrument position, which will not necessarily correspond to the vertical at which the maximum velocity in a cross-section occurs. This overcomes the problem due to the fact that the maximum velocity continuously modifies its position in time with changing cross-section shape and current characteristics.

As a final remark, it must be stated that the gauging site of Tavagnasco was selected as a test case for the evaluation of the proposed approach because a steady-flow rating curve was already available. When establishing a new gauging site, several measurements of discharge using conventional approaches such as current meters or ADCPs will be

required in order to develop an initial steady-state rating curve to calibrate the proposed approach.

## REFERENCES

- Ammari, A. & Remini, B. 2010 Estimation of Algerian rivers discharges based on Chiu's equation. *Arab Journal of Geoscience* 3, 59–65.
- Ardiclioglu, M., de Araújo, J. C. & Senturk, A. I. 2005 Applicabilità des Equations de Distribution de Vitesses dans les Ecoulements en Canal Ouvert à fond rugueux. *La Houille Blanche* 4, 73–79 (in French).
- Barbetta, S., Melone, F. & Moramarco, T. 2002 Sull'accuratezza dei metodi di stima delle scale di deflusso, *Proc. XXVIII Convegno Nazionale di Idraulica e Costruzioni Idrauliche*, Potenza, Vol. III, pp. 566–570 (in Italian).
- Barnes Jr., H. H. 1967 Roughness characteristics of natural channels. US Geological Survey Water-Supply Paper 1849, 213 pp.
- Brocca, L., Corato, G., Corradini, C., Melone, F. & Moramarco, T. 2010 Stima della velocità media in canali naturali attraverso il monitoraggio della velocità massima superficiale. *Atti XXXII Convegno Nazionale di Idraulica e Costruzioni Idrauliche*, Palermo (in Italian).
- Burnelli, A., Moramarco, T. & Saltalippi, C. 2006 Valutazione dei profili di velocità in canali naturali per eventi di piena eccezionali. *Proc. XXX Convegno di Idraulica e Costruzioni Idrauliche*, Rome (in Italian).
- Chiu, L. C. 1987 Entropy and probability concepts in hydraulics. *Journal of Hydraulic Engineering* 113 (5), 583–600.
- Chiu, L. C. 1988 Entropy and 2-D velocity in open channels. *Journal of Hydraulic Engineering* 114 (7), 738–756.
- Chiu, L. C. 1989 Velocity distribution in open channels. *Journal of Hydraulic Engineering* 115 (5), 576–594.
- Chiu, L. C. 1991 Application of entropy concept in open channel flow study. *Journal of Hydraulic Engineering* 117 (5), 615–628.

- Chiu, C. L. & Murray, D. W. 1992 Variation of velocity distribution along non-uniform open-channel flow. *Journal of Hydraulic Engineering* **118** (7), 989–1001.
- Chow, V.-T. 1958 *Open Channel Hydraulics*. McGraw-Hill, Tokyo.
- Chiu, C. L. & Abidin Said, C. A. 1995 Maximum and mean velocities and entropy in open-channel flow. *Journal of Hydraulic Engineering* **121** (1), 26–35.
- Costa, J. E., Cheng, R. T., Haeni, F. P., Melcher, N., Spicer, K. R., Hayes, E., Plant, W., Hayes, K., Teague, C. & Barrick, D. 2006 Use of radars to monitor stream discharge by noncontact methods. *Water Resources Research* **42**, 1–14.
- de Araùjo, J. C. & Chaudhry, F. H. 1998 Experimental evaluation of 2-D entropy model for open-channel flow. *Journal of Hydraulic Engineering* **124** (10), 1064–1067.
- Di Baldassarre, G. & Montanari, A. 2009 Uncertainty in river discharge observations: a quantitative analysis. *Hydrology and Earth System Sciences* **13**, 913–921.
- Dottori, F., Martina, M. V. L. & Todini, E. 2009 A dynamic rating curve approach to indirect discharge measurement. *Hydrology and Earth System Sciences* **13**, 847–863.
- Ferro, V. 2003 ADV measurements of velocity distributions in a gravel-bed flume. *Earth Surface Processes and Landforms* **28**, 707–722.
- Ferro, V. & Baiamonte, G. 1994 Flow velocity profiles in gravel-bed rivers. *Journal of Hydraulic Engineering* **120** (1), 60–80.
- Fulton, J. & Ostrowski, J. 2008 Measuring real-time streamflow using emerging technologies: radar, hydro-acoustics, and the probability concept. *Journal of Hydrology* **357**, 1–10.
- Greco, M. 1999 Entropy velocity distribution in a river. *Proceedings of IAHR Symposium on River, Coastal and Estuarine Morphodynamics*. IAHR, Delft, The Netherlands, 2, pp. 121–130.
- Greco, M. & Mirauda, D. 1999 Downward and upward approach for entropy velocity profile. In: *Hydraulic Modeling. Proceedings of 2nd International Conference on Water, Environment, Ecology, Socio-economics and Health Engineering* (V. P. Singh, I. Seo & J. H. Sonu, eds). Water Resources Publications, LLC, Highlands Ranch, CO, pp. 123–132.
- Moramarco, T. & Singh, V. P. 2001 Simple method for relating local stage and remote discharge. *Journal of Hydrologic Engineering* **6** (1), 78–81.
- Moramarco, T. & Saltalippi, C. 2002 Stima della velocità media in sezioni di un corso d'acqua naturale. *Atti XXVIII Convegno di Idraulica e Costruzioni Idrauliche, Potenza III*, 263–274 (in Italian).
- Moramarco, T. & Singh, V. P. 2008 Streamflow measurements and discharge assessment during high flood events. In *Hydrology and Hydraulics* (V. P. Singh, ed.). Water Resources Publications, Highlands Ranch, Colorado, pp. 899–942.
- Moramarco, T., Ammari, A., Burnelli, A., Mirauda, D. & Pascale, V. 2008 Entropy theory application for flow monitoring in natural channels. In: *Proceedings of iEMSs 4th Biennial Meeting: International Congress on Environmental Modelling and Software (iEMSs 2008)* (M. Sánchez-Marrè, J. Béjar, J. Comas, A. E. Rizzoli & G. Guariso, eds). International Environmental Modelling and Software Society, Barcelona, Spain, pp. 430–437.
- Moramarco, T., Saltalippi, C. & Singh, V. S. 2004 Estimation of mean velocity in natural channels based on Chiu's velocity distribution equation. *Journal of Hydraulic Engineering* **9** (1), 42–50.
- Moramarco, T., Saltalippi, C. & Singh, V. P. 2011 Velocity profiles assessment in natural channels during high floods. *Hydrology Research* **42** (2–3), 162–170.
- Rantz, S. E. et al. 1982 Measurement and computation of streamflow: Vol. 1, Measurement of stage and discharge; Vol. 2 Computation of discharge. US Geological Survey. Water-Supply Paper 2175.
- Stephan, U. & Gutknecht, D. 2002 Hydraulic resistance of submerged flexible vegetation. *Journal of Hydrology* **269**, 27–43.
- Xia, R. 1997 Relation between mean and maximum velocities in a natural river. *Journal of Hydraulic Engineering* **123** (8), 720–723.
- Yamaguchi, T. & Niizato, K. 1994 Flood discharge measurement using radio current meters. *Journal of the Japan Society of Civil Engineers* **497** (II-28), 41–50 (in Japanese).
- Zasso, M. 2010 Ricostruzione dei profili di velocità per la restituzione di misure correntometriche condotte in condizioni di piena. Azienda Regional per la Prevenzione e la Protezione Ambientale del Veneto, ARPAV, Report n. 01/2010 (in Italian).

Copyright of Hydrology Research is the property of IWA Publishing and its content may not be copied or emailed to multiple sites or posted to a listserv without the copyright holder's express written permission. However, users may print, download, or email articles for individual use.



Copyright of Hydrology Research is the property of IWA Publishing and its content may not be copied or emailed to multiple sites or posted to a listserv without the copyright holder's express written permission. However, users may print, download, or email articles for individual use.